MSH2–MSH6 stimulates DNA polymerase η, suggesting a role for A:T mutations in antibody genes

Teresa M. Wilson,[1] Alexandra Vaisman,[2] Stella A. Martomo,[3] Patsa Sullivan,[1] Li Lan,[4] Fumio Hanaoka,[5,6] Akira Yasui,[4] Roger Woodgate,[2] and Patricia J. Gearhart[3]

[1]Radiation Oncology Research Laboratory, Department of Radiation Oncology, University of Maryland, Baltimore, MD 21201
[2]Section on DNA Replication, Repair and Mutagenesis, Laboratory of Genomic Integrity, National Institute of Child Health and Human Development, National Institutes of Health (NIH), Bethesda, MD 20892
[3]Laboratory of Molecular Gerontology, National Institute on Aging, Bethesda, MD 20892
[4]Department of Molecular Genetics, Institute of Development, Aging and Cancer, Tohoku University, Sendai 980-8575, Japan
[5]Graduate School of Frontier Biosciences, Osaka University, Osaka 565-0871, Japan
[6]Discovery Research Institute, RIKEN and Core Research for Evolutional Sciences and Technology, Japan Science and Technology Corporation, Saitama 351-0198, Japan

Activation-induced cytidine deaminase deaminates cytosine to uracil (dU) in DNA, which leads to mutations at C:G basepairs in immunoglobulin genes during somatic hypermutation. The mechanism that generates mutations at A:T basepairs, however, remains unclear. It appears to require the MSH2–MSH6 mismatch repair heterodimer and DNA polymerase (pol) η, as mutations of A:T are decreased in mice and humans lacking these proteins. Here, we demonstrate that these proteins interact physically and functionally. First, we show that MSH2–MSH6 binds to a U:G mismatch but not to other DNA intermediates produced during base excision repair of dUs, including an abasic site and a deoxyribose phosphate group. Second, MSH2 binds to pol η in solution, and endogenous MSH2 associates with the pol in cell extracts. Third, MSH2–MSH6 stimulates the catalytic activity of pol η in vitro. These observations suggest that the interaction between MSH2–MSH6 and DNA pol η stimulates synthesis of mutations at bases located downstream of the initial dU lesion, including A:T pairs.

CORRESPONDENCE
Patricia J. Gearhart:
gearhartp@grc.nia.nih.gov

Abbreviations used: AID, activation-induced cytidine deaminase; dRP, 5′-deoxyribose phosphate; dU, uracil; pol, polymerase; GST, glutathione *S*-transferase; UNG, dU glycosylase.

Somatic hypermutation generates substitutions in Ig variable genes and switch regions before heavy chain constant genes at an astounding frequency of 10^{-2} mutations per basepair. The mutation pathway is initiated by the activation-induced cytidine deaminase (AID) protein, which is only expressed in B cells (1, 2). AID deaminates cytosine on single-stranded DNA substrates to generate uracil (dU) in vitro (3–9), and these dUs could generate mutations of C:G pairs in three ways. First, dU might be copied by a high fidelity polymerase (pol) that inserts A opposite U to produce C to T transitions (10). Second, dU could be removed by dU glycosylase (UNG) to produce an abasic site (11–13), which is repaired during base excision repair by a low fidelity pol to produce mutations at the site of the deaminated C (14). Third, dU could be removed by UNG, and the abasic site is copied by a translesion pol to generate mutations opposite the site (15). Thus, dU or an abasic lesion produces mutation at C bases, or at G bases if C is deaminated on the complementary strand. Indeed, mutations of C:G are predominantly observed when AID is overexpressed in bacteria (10), yeast (16), fibroblast cells (17), B cell lines (18, 19), and transgenic mice (20). However, the spectrum of mutation in antibody genes from mice and men includes mutations of A:T as frequently as mutations of C:G, indicating that other proteins (21), besides AID, participate in the mutation pathway.

Among these proteins, the mismatch repair MSH2–MSH6 heterodimer and DNA pol η have been implicated in hypermutation. Ig variable and switch regions from mice deficient for Msh2 and Msh6 have the same frequency of mutation as wild-type mice, but have fewer mutations of A:T and correspondingly higher mutations of C:G (22–29). MSH2–MSH6 must have a specialized function in hypermutation that is separate from canonical mismatch repair because mice deficient for other proteins

in the repair pathway, Msh3, Pms2, and Mlh1, do not have a strong bias for mutations of C:G in Ig genes (24, 26, 30–33).

Similarly, humans with the xeroderma pigmentosum variant disease, who are deficient in the low fidelity DNA pol η, have a normal frequency of hypermutation in variable and switch regions but fewer mutations of A:T (34–36). In agreement with the genetic data, pol η has been shown to increase the frequency of substitutions of A:T basepairs on DNA substrates in vitro in a manner that corresponds to variable gene mutation (37, 38). However, mice deficient for other low fidelity DNA pols, such as β, ζ, ι, κ, λ, and μ, have no discernible change in the types of substitutions (39–43), indicating that these pols either do not participate in hypermutation or their role is nonessential.

Because animals deficient for MSH2–MSH6 and pol η exhibit the same phenotype of fewer mutations of A:T, we considered the possibility that they may operate together in the same branch of the hypermutation pathway. Our studies revealed that MSH2–MSH6 not only binds to a U:G mispair, but also physically interacts with pol η and functionally stimulates its catalytic activity.

RESULTS

MSH2–MSH6 binds to a U:G mismatch but not to an abasic site or a 5′-deoxyribose phosphate (dRP) group

MSH2–MSH6 might be recruited into the hypermutation process by binding to an AID-induced U:G mispair or to a DNA intermediate that would be produced during base excision repair. To test these possibilities, we generated DNA substrates containing a U:G mismatch, an abasic site produced by the removal of U with UNG, and a dRP group produced by nicking of the abasic site by an endonuclease. For control substrates, homoduplex DNA was used as a negative control, and T:G heteroduplex DNA was used as a positive control. We assessed the ability of increasing amounts of purified human MSH2–MSH6 to form complexes with each of the DNA substrates by a gel mobility shift assay (Fig. 1). MSH2–MSH6 bound to the U:G mismatch (K_d = 30.5 ± 0.6 nM) with about half of the affinity as for the control T:G mismatch (K_d = 18.9 ± 0.6 nM). MSH2–MSH6 did not bind to an abasic site or dRP lesion in this assay, nor did MSH2–MSH3 bind to a U:G substrate (not depicted). Although binding of MSH2–MSH6 to a U:G-containing substrate has been reported previously (44), these data present a systematic analysis of binding to various intermediates in the base excision repair pathway. The results suggest that MSH2–MSH6 can enter the hypermutation pathway by recognizing an AID-induced U:G mispair or by binding to a T:G mispair generated during error-prone base excision repair of dU (14).

MSH2 binds to pol η

Several techniques were used to detect an interaction between the mismatch repair proteins and pol η. First, an ELISA assay was used to see if the pol bound to intact MutS complexes. As shown in Fig. 2, pol η bound to both MSH2–MSH3 and MSH2–MSH6 that were immobilized on plastic microtiter plates, but not to BSA. The data were analyzed by a Hill plot, and the apparent dissociation constant (K_d) for pol η binding to MSH2–MSH3 was 7.4 ± 1.0 nM, and to MSH2–MSH6 was 6.5 ± 0.8 nM.

Second, pull-down experiments were performed with the individual proteins to detect physical interactions in solution. The control for these reactions was pol ι, which has been hypothesized to participate in hypermutation in a cell line (45). COOH-terminal fragments comprising the last 233 amino acids of human pol η and 224 amino acids of human pol ι were expressed as glutathione *S*-transferase (GST) fusion proteins in bacteria (Fig. 3 A). Individual subunits of the human MutS proteins, MSH2, MSH3, and MSH6, were translated in vitro with [^{35}S]methionine and incubated with beads coupled with either GST alone, GST–C-terminal pol η, or GST–C-terminal pol ι. As shown in Fig. 3 B, the most efficient coprecipitation was between GST–pol η and MSH2, where 47% of the input MSH2 was pulled down in the assay, but there was also significant binding of GST–pol η to MSH3 and MSH6. GST–pol ι also bound to MSH2 and MSH3, but at a much lower level, and there was no interaction between the DNA pols and GST alone.

Third, coimmunoprecipitations with anti-FLAG antibody were performed using extracts from HeLa cells that

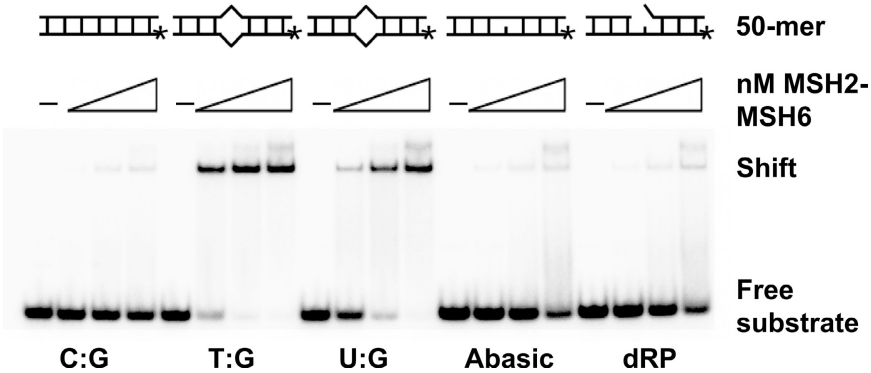

Figure 1. The MSH2–MSH6 heterodimer binds to a U:G mismatch. Increasing amounts of the MSH2–MSH6 complex (0–60 nM) were incubated with 1 fmol of the various labeled 50-mer DNA substrates, which are depicted at the top of the figure. Bound complexes were detected by a shift in the substrate after electrophoresis.

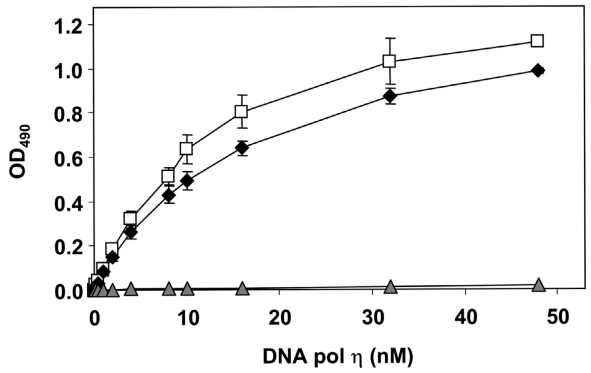

Figure 2. Pol η binds to MSH2–MSH3 and MSH2–MSH6 heteroduplexes by ELISA analysis. Wells were coated with MSH2–MSH3 (diamonds), MSH2–MSH6 (squares), or BSA (triangles) and incubated with increasing amounts of pol η. Bound protein was detected with anti–pol η antibody.

were stably transfected with a vector that overexpressed FLAG-tagged pol η or with FLAG vector alone. As seen in Fig. 3 C, Western blot analyses of the FLAG immunoprecipitates with anti-MSH2 antibodies showed that ~12% of the input MSH2 could be precipitated from cell extracts expressing FLAG–pol η. MSH2 did not precipitate with the FLAG vector alone or with FLAG-XRCC1 (not depicted), which is not involved in mismatch repair or translesion synthesis. This demonstrates that endogenous MSH2 interacts with overexpressed pol η in vivo.

MSH2–MSH6 stimulates pol η replication

In vitro primer extension assays were performed to determine if MSH2–MSH6 altered the ability of pol η to synthesize DNA. Preliminary experiments revealed that DNA synthesis by pol η was similar on both recessed primer and one base–gapped templates (not depicted). Recessed primer substrates were used for all subsequent experiments because they would resemble Ig substrates if long gaps were introduced by exonuclease activity near the AID lesion. Fig. 4 A shows the effect of mismatch repair proteins on pol η synthesis, using a DNA template with dA as the first available base. Although the addition of MSH2–MSH3 had no obvious effect on primer elongation by pol η, the addition of MSH2–MSH6 appeared to stimulate the activity of pol η. In contrast, MSH2–MSH6 did not alter the ability of pol ι to elongate primers (Fig. 4 B). The extent of stimulation of pol η varied over a range of enzyme concentrations, and primer elongation was quantified by a PhosphorImager and calculated as percent of total primer termini. Stimulation was greatest at 14 nM enzyme, where primer extension increased 10-fold, and was about twofold greater on substrates with A or T as the first template base to be copied, compared with when it was G or C (Fig. 4, A and

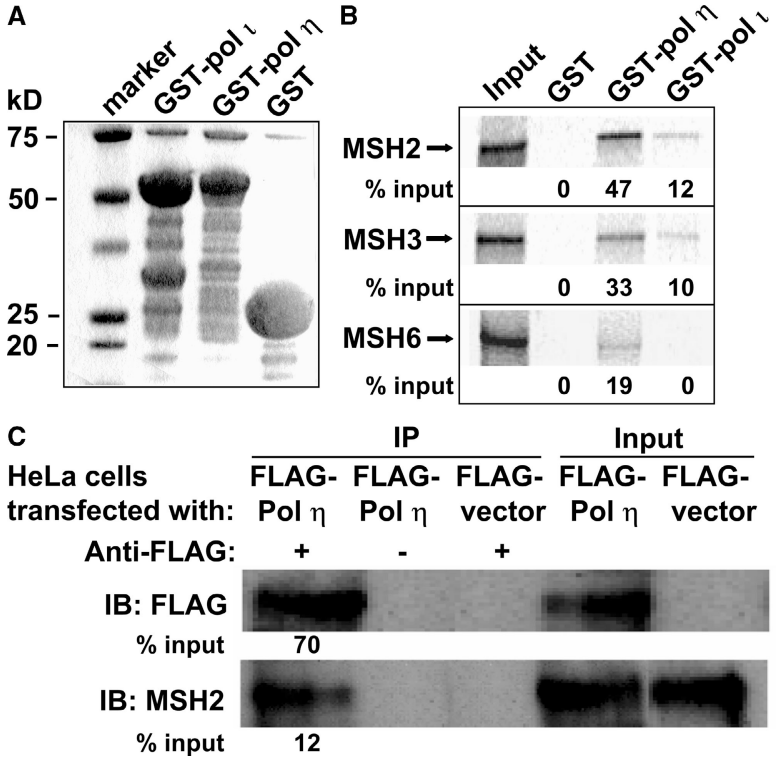

Figure 3. Pol η interacts with MSH2 in vitro and in vivo. (A) Coomassie-stained gel. An SDS-PAGE gel shows the purity of the GST-tagged COOH-terminal pols before they were coupled to glutathione-Sepharose beads. (B) GST pull-down assay. ^{35}S-labeled MSH2, MSH3, and MSH6 proteins were incubated with the pol-coupled beads and resolved on an SDS-PAGE gel. Input lanes represent 100% of the MSH protein added to the assay tube. (C) Immunoprecipitation. FLAG-tagged pol η was overexpressed in HeLa cells and immunoprecipitated (IP) with or without antibody to FLAG protein. Precipitates were solubilized and separated by electrophoresis. The gel was immunoblotted (IB) for Western analyses using an antibody to FLAG to detect pol η and an antibody to MSH2. Input lanes represent 30% of the cell extracts used in the assay.

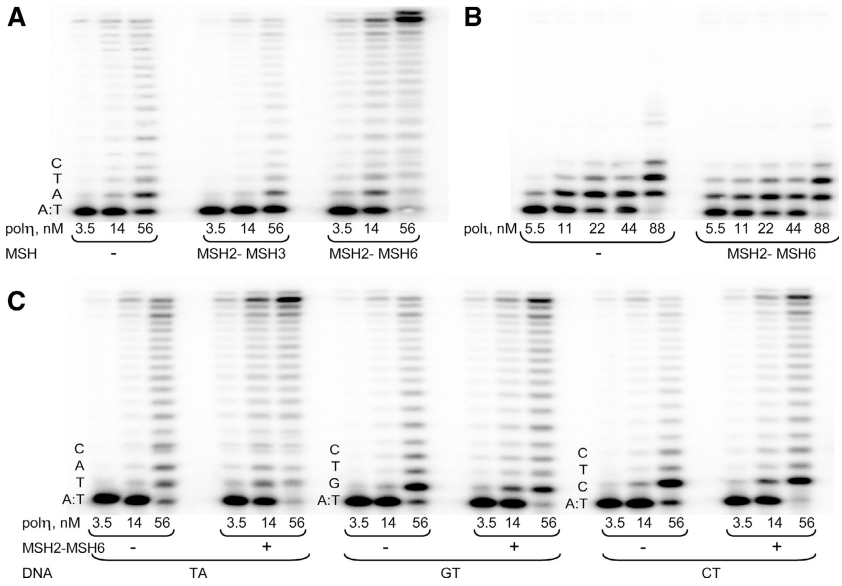

Figure 4. Effect of mismatch repair proteins on DNA replication by pols η and ι. All reactions were performed for 10 min. (A) Dose–response experiments depicting pol η–catalyzed primer extension in the presence of MSH2–MSH3 or MSH2–MSH6 with AT as the first two template bases to be copied. (B) Dose–response experiments depicting pol ι–catalyzed primer extension in the presence of MSH2–MSH6 using the same template as in A. (C) Influence of template sequence context on the MSH2–MSH6-dependent stimulation of primer extension by pol η. TA, GT, and CT represent the first two bases to be copied.

C). The MSH2–MSH6 complex also enhanced the ability of pol η to extend T:G and U:G mispaired primer termini, although the amount of extended products at different pol η concentrations was ~3–20-fold less than with the correctly paired C:G termini (Fig. 5). It should be noted that the length of the 18-mer primer and 40-mer template might be too short for MSH2–MSH6 to bind to the mispaired termini, and the observed stimulation might be through protein–protein interactions of the pol and repair complex.

Pol η is a distributive enzyme and incorporates only a few nucleotides before dissociating from the extended product (46, 47). To determine the mechanism of how MSH2–MSH6 stimulates the activity of pol η, we tested the effect of the complex on processivity and fidelity of the pol. Processivity, or the extent to which the pol elongates a primer in a single encounter with the substrate, was measured in the presence of a DNA trap. Under these conditions, pol molecules that dissociate from the radiolabeled DNA primer/template

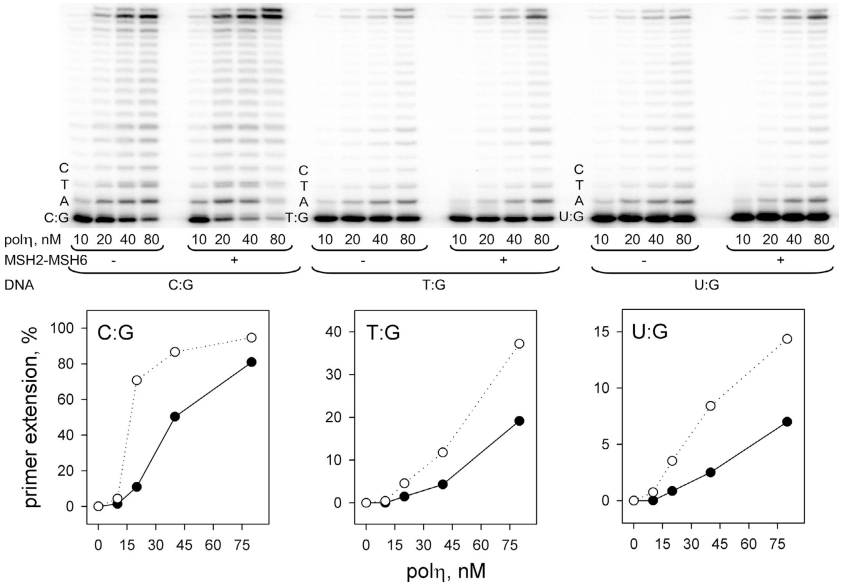

Figure 5. MSH2–MSH6 dependent stimulation of primer extension by pol η using matched (C:G) and mismatched (T:G or U:G) termini. All reactions were performed for 10 min. The graphs indicate quantitation of the gels and plot primer elongation catalyzed by pol η alone (closed circles) or in the presence of MSH2–MSH6 (open circles) as a percentage of total primer termini.

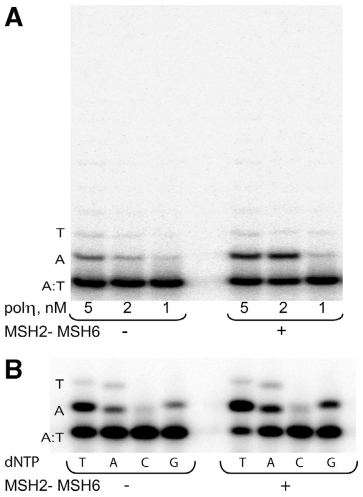

Figure 6. Effect of MSH2–MSH6 on processivity and fidelity of pol η. The local template sequence is shown to the left of each set of gels. (A) Processivity of pol η was measured in the absence and presence of MSH2–MSH6 in two-min reactions containing all four nucleotides and herring sperm DNA as a trap for pol molecules that dissociate from the radiolabeled primer template. (B) Nucleotide incorporation specificity of pol η in the absence and presence of MSH2–MSH6 was measured in 10-min reactions containing 100 μM of each individual nucleotide.

are trapped by binding to excess nonlabeled DNA. As shown in Fig. 6 A, the processivity of pol η did not change upon the addition of MSH2–MSH6, and only one nucleotide was predominantly incorporated by the pol before dissociating from the DNA template. Fidelity was assessed by primer extension assays in the presence of individual nucleoside triphosphates. As shown in Fig. 6 B, MSH2–MSH6 did not change the overall fidelity of pol η because the amount of A and G misincorporation opposite template A was similar in the presence and absence of the MSH complex.

To understand how MSH2–MSH6 stimulates the catalytic activity of pol η without changing its processivity or fidelity, we performed steady-state kinetic analyses of incorporation opposite template dA using standing start reaction conditions where nucleotide insertion is measured at the first template site adjacent to the original primer 3′ terminus (48). Although the absolute values of kinetic parameters V_{max} and K_m derived from the standing start assay have limited mechanistic significance, the ratios of V_{max}/K_m should be a reliable measure of the effect of MSH2–MSH6 on pol activity. V_{max} is a measure of the catalytic rate of the reaction, although it also could be a measure of product release, whereas K_m most likely measures the affinity of the pol for the dNTP substrate (48). In the presence of MSH2–MSH6, the V_{max} increased sixfold, and the K_m increased 2.5-fold (Table I). As a result, the catalytic efficiency of nucleotide incorporation (V_{max}/K_m) by pol η increased ~2.3-fold. It should be noted that despite the slight increase in K_m, the dNTP concentrations used in the primer extension experiments, as well as the dNTP levels in cell nuclei (49), are higher than the apparent K_m determined here. Thus, the increased catalytic activity of pol η is largely due to the effect of the MSH2–MSH6 complex on the V_{max} or rate of reaction.

Table I. Kinetic analysis of dTTP incorporation opposite template A as catalyzed by pol η in the absence or presence of MSH2–MSH6[a]

	V_{max} (%$^{-1}$ min^{-1})	K_m (μM)	V_{max}/K_m
Without MSH2–MSH6	3.8 ± 0.6	2.6 ± 0.2	1.4 ± 0.2
With MSH2–MSH6	22.5 ± 5.3	6.7 ± 0.7	3.3 ± 0.6

[a]Data are means (± standard error) from three to five experiments. V_{max}/K_m values are the percentage of primer elongation product per min per μmol of nucleotide.

DISCUSSION

Interactions between the MSH2–MSH6 heterodimer and DNA pol η are of interest because animals deficient for these proteins have similar phenotypes of fewer mutations of A:T basepairs in Ig genes, which suggests that they operate together during hypermutation. In this study, we examined whether these proteins physically interact and if the interaction affects pol activity. Three different assays were used to demonstrate binding of the mismatch repair proteins to pol η. First, intact MSH2–MSH3 and MSH2–MSH6 complexes bound avidly to pol η in an ELISA assay. Second, to determine which MSH subunit interacted with pol η, the proteins were individually labeled and incubated with purified COOH-terminal fragments of pols η and ι fused to GST. As analyzed in a pull-down assay, pol η exhibited strong binding to MSH2 and weak binding to MSH3 and MSH6, and pol ι had much weaker binding to MSH2 and MSH3. Third, in HeLa cell extracts, FLAG-tagged pol η coprecipitated with endogenous MSH2, demonstrating that the two proteins are likely to associate in living cells.

To test for a functional interaction between the protein complexes, the ability of pol η to elongate a recessed primer template was measured after the addition of MSH2–MSH6 or MSH2–MSH3 heterodimers. MSH2–MSH6 stimulated synthesis largely by increasing the V_{max} of the reaction, but did not alter the processivity or fidelity of the enzyme in these assays. In contrast, although the ELISA and pull-down experiments suggested that pol η and MSH2–MSH3 physically interact, MSH2–MSH3 did not affect pol η activity. Likewise, although the pull-downs showed some interaction between pol ι and MSH2, MSH2–MSH6 did not stimulate pol ι synthesis.

Although we cannot exclude the possibility that interaction with MSH2–MSH6 simply stabilizes pol η in vitro, leading to a stimulation of its catalytic activity, our data support the hypothesis that these proteins work together during somatic hypermutation to produce mutations downstream of the initial dU lesion at all four bases, including A and T. One possible scenario is that MSH2–MSH6 first binds to U:G mismatches that are generated by AID, and then attracts pol η and other proteins to the site. However, for pol η to synthesize DNA, a nick must first be generated in the nontemplate DNA to allow access of the pol to a 3′ primer ter-

minus. There is compelling evidence that the nick is not due to an endonuclease cleaving at an abasic site that would be produced after the removal of dU by UNG because *ung*$^{-/-}$ mice and humans have normal frequencies of substitutions of A:T (12, 13). Therefore, mutations of A:T pairs can be produced in the absence of UNG and do not require an abasic site for the mechanism. Nicks might be generated in the vicinity of the U:G mispair by an endonuclease associated with MSH2, such as ERCC1-XPF (50, 51) or YB-1 (52). MSH2 also binds to exonuclease 1 (53), which would produce a gap at the nick and provide access for pol η to synthesize DNA (54). Alternatively, in a wild-type background, MSH2–MSH6 might bind to a T:G mispair that has been erroneously generated during short patch base excision repair of the deaminated cytosine. This may recruit pol η to the primer terminus, where it extends the repair patch through strand displacement (43). In either case, as error-prone synthesis by pol η occurs, mismatches will be generated opposite neighboring bases. Repeated cycles of MSH2–MSH6 binding to the mismatches would further stimulate pol η to make more mutations in the vicinity of the original cytosine deamination. Further experiments are necessary to clarify the exact mechanism of how pol η generates mutations of A:T, but it is clear that MSH2–MSH6 plays a central role in the process because mice deficient for both UNG and Msh2 have only mutations of C:G and no mutations of A:T (55).

MATERIALS AND METHODS

Proteins. Human proteins were used in all of the experiments. MSH2–MSH6 and MSH2–MSH3 complexes were purified from a baculovirus insect cell system essentially as described previously (56). For the MSH2–MSH6 complex, the following modifications were performed: peak fractions eluted from the PBE 94 column were combined and the NaCl concentration was adjusted to 200 mM with buffer B (50 mM NaCl, 25 mM Hepes-NaOH, pH 7.9, 1 mM DTT, 0.1 mM EDTA, 10% glycerol, and protease inhibitors). The sample was then loaded onto a Resource Q column (Amersham Biosciences) preequilibrated with buffer B containing 200 mM NaCl and eluted with linear gradient of NaCl from 200 mM to 1 M. The MSH2–MSH6 complex eluted at ∼450 mM NaCl. The protein fractions were dialyzed and quantified as described previously (57). The MSH2–MSH6 and MSH2–MSH3 pFastBac Dual expression constructs were provided by R. Fishel (Thomas Jefferson University, Philadelphia, PA).

For GST pull-down assays, GST-tagged COOH-terminal pols η and ι were made by fusing GST to the COOH-terminal 233 amino acids of pol η (full-length = 713 amino acids) or the COOH-terminal 224 amino acids of pol ι (full-length = 715 amino acids). GST-tagged pol η was expressed in *Escherichia coli* from plasmid pWC9 and was constructed by PCR amplification of the 3′ end of pol η cDNA (58) using the following primers: 5′-GCTAGAAGAATTCTCTAAAGCAACTCCTGC-3′ and 5′-AGGCACAGTCGAGGCTGATCAGCGG-3′. The PCR amplicon was digested with EcoRI and DraI, and the 414-bp product was cloned into the EcoRI–SmaI-digested GST expression vector, pGEX-4T-1 (Amersham Biosciences). GST-tagged pol ι was expressed from plasmid pAR208, whose construction has been described elsewhere (59). The plasmids were transformed into *E. coli* BL21λDE3 and induced by the addition of 1 mM isopropyl β-D-thiogalactopyranoside (Sigma-Aldrich). GST-tagged proteins were bulk purified using glutathione sepharose beads (Amersham Biosciences) according to the manufacturer's instructions. Labeled MSH2, MSH3, and MSH6 proteins were prepared from pET28a expression vectors that each contained genes for the three proteins. The vectors were transcribed and translated in vitro using a TNT Coupled Reticulocyte Lysate System (Promega) in the presence of [^{35}S]methionine (Amersham Biosciences).

For the ELISA and pol replication assays, recombinant human pol η, tagged with $(His)_6$ at its COOH-terminal end, was expressed in Sf9 insect cells using the baculovirus expression system and prepared as described by Masutani et al. (47). GST-tagged pol ι was purified from baculovirus-infected insect cells as described previously (60).

ELISA assays. Wells were coated with 500 fmol of either BSA, MSH2–MSH3, or MSH2–MSH6 proteins diluted in carbonate buffer containing 0.016 M Na_2CO_3 and 0.034 M $NaHCO_3$, pH 9.8, overnight at 4°C. After removal of the proteins, the wells were coated with blocking buffer containing 3% BSA and 0.1% TWEEN 20 diluted in PBS and incubated for 1 h at room temperature. The wells were washed with washing buffer containing 0.1% TWEEN 20 in PBS. Serial dilutions of pol η in blocking buffer were then added to each well and incubated at room temperature for 1 h. After washing the wells with washing buffer, rabbit antibody to COOH-terminal pol η was diluted at 1:500 in blocking buffer, added to each well, and incubated for 1 h. The wells were then washed with washing buffer three times. Goat anti–rabbit IgG antibody conjugated to horseradish peroxidase (Vector Laboratories) was diluted at 1:5,000 in blocking buffer, added to each well for 1 h, and the wells were washed five times with washing buffer. Bound antibody was detected with *o*-phenylenediamine dihydrochoride followed by termination with 3M H_2SO_4, and the absorbance was read at 490 nm. Data were analyzed using the Hill plot according to a method published previously (61).

Gel mobility shift assays. For generation of DNA substrates containing a T:G or U:G mismatch, 50-mer oligonucleotides of the following sequences were obtained from Invitrogen: top strand (5′-CATTATCCTAAACATAACTTAACTAG**X**TTAACTTAATTCTTCAATATACC-3′) and bottom strand (5′-GGTATATTGAAGAATTAAGTTAAGCTAGTTAAGTTATGTTTAGGATAATG-3′). For the homoduplex substrate, **X** = C; for T:G, **X** = T; and for U:G, **X** = U. The bottom strand oligonucleotide was 5′ end labeled using γ[^{32}P]-ATP and T4 polynucleotide kinase, followed by purification through a ProbeQuant column (Amersham Biosciences). The labeled strand was then annealed to an equimolar amount of top strand containing C, T, or U. To generate the abasic and dRP substrates, the duplex U:G mismatched substrate was incubated with UNG and UNG/Endo IV, respectively, for 20 min at 37°C. The substrates were then purified by centrifugation through a ProbeQuant column. The DNA binding assays were performed by incubating increasing concentrations (0, 15, 30, and 60 nM) of the MSH2–MSH6 heterodimer with 1 fmol of the ^{32}P-labeled DNA substrates in a buffer containing 100 mM NaCl, 25 mM Hepes-NaOH, pH 7.9, 1 mM DTT, 0.5 mM $MgCl_2$, 0.1 mM ADP, 10% glycerol, 75 μg/ml BSA, and 1 pmol of a 200-bp homoduplex competitor in a final reaction volume of 20 μl. The reactions were incubated at 37°C for 20 min followed by electrophoresis on a 5% polyacrylamide (29:1, acrylamide/bisacrylamide) gel for 1.5 h at 4°C. The gels were dried, visualized using a Bio-Rad Laboratories Personal fx PhosphorImager, and the percent "free" versus "protein-bound" DNA was quantified using ImageQuant software. To determine the apparent dissociation constant (K_d) values, nonlinear regression (curve fit) was performed using GraphPad Prism version 4.00 for Windows.

GST pull-down assays. GST-tagged COOH-terminal pols η and ι or GST alone was coupled to glutathione sepharose beads and mixed with either ^{35}S-labeled MSH2, MSH3, or MSH6 in binding buffer (PBS, 0.2% Triton-X 100, 5% BSA and protease inhibitor; complete protease inhibitor cocktail; Boehringer) for 30 min at room temperature. The beads were washed twice in binding buffer without BSA. The bound proteins were separated on a 4–15% linear gradient Tris-HCl gel (SDS-PAGE; Bio-Rad Laboratories) and visualized with a PhosphorImager.

Immunoprecipitation from HeLa cell extracts. HeLa cells were stably transfected either with a plasmid containing the human pol η gene

tagged with a FLAG epitope expressed by a chicken β actin promoter (62), or with a plasmid containing the FLAG vector alone. Cells were lysed in TNE buffer (10 mM Tris-HCl, pH 7.8, 1% NP-40, 0.15 M NaCl, and 1 mM EDTA) supplemented with protease inhibitors for 30 min on ice. The suspensions were centrifuged at 15,000 rpm for 15 min at 4°C. Supernatants were then collected and protein concentrations were determined. For immunoprecipitation, 1 mg of protein was mixed with Dynabeads (Dynal) coupled to anti–mouse IgG to preclear the lysate. The lysate was then incubated overnight with or without 1 μg mouse anti-FLAG antibody. The solution was added to the beads for an overnight incubation and then washed with TNE buffer five times at 4°C to remove nonspecific proteins. For Western blotting, the samples were resuspended in loading buffer, boiled for 5 min, and centrifuged. 40 μg of the supernatant protein was loaded into each lane of a 4–20% SDS polyacrylamide gel and subjected to electrophoresis. Proteins were then transferred to a PVDF membrane and stained with a 1:1,000 dilution of antibodies to FLAG (Sigma-Aldrich) and MSH2 (Santa Cruz Biotechnology, Inc.) and detected by ECL-enhanced chemiluminescence (Amersham Biosciences).

Primer extension assays. The sequence of the 40-mer oligonucleotide templates used in most primer extension experiments is 5′-AGCGTCTTAATCTAAGC**YX**TCGCTATGTTTTCAAGGATTC-3′, where **X** is either T, A, G, or C, and **Y** is either T or A. The sequence of the 18-mer primer was 5′-TCCTTGAAAACATAGCGA-3′. The sequence of the 40-mer oligonucleotide template used in the mismatch extension experiments is 5′-AGCGTCTTAATCTAAGCTAGCTCGATGTTTTCAAGGATTC-3′, and the sequence of the 18-mer primers is 5′-TCCTTGAAAACATCGAG**X**-3′, where **X** is either C, T, or U.

All primers and templates were synthesized by Loftstrand Laboratories using standard techniques and were gel purified before use. Primers were 5′ end labeled using T4 polynucleotide kinase and γ[^{32}P]-ATP. DNA substrates were prepared by annealing templates with ^{32}P-labeled primers at a 1.5:1 molar ratio. Hybridization was achieved by heating the required mixture of oligonucleotides in an annealing buffer (50 mM Tris-HCl, pH 8, 5 mM $MgCl_2$, 50 μg/ml BSA, and 1.42 mM 2-mercaptoethanol) for 10 min at 100°C followed by slow cooling to room temperature over a period of ~2 h. Annealing efficiencies were >95%, as evidenced by the different mobility of the ^{32}P-labeled primers before and after hybridization to the template on nondenaturing polyacrylamide gels. 10 nM primer template (expressed as primer termini) was incubated with DNA pol η or pol ι at 37C° for 10 min in 10-μl reactions containing 100 μM of either all four dNTPs (for primer extension assays) or each dNTP individually (for fidelity assays), 40 mM Tris-HCl, pH 8.0, 5 mM $MgCl_2$, 10 mM dithiothreitol, 250 μg/ml BSA, and 2.5% glycerol in the presence or absence of 150 nM MSH2–MSH3 or MSH2–MSH6 complex. Reactions catalyzed by pol η also contained 60 mM KCl. Enzyme concentrations are indicated in the figures. Reactions were terminated by mixing with 10 μl formamide loading dye solution containing 50 mM EDTA, 0.1% xylene cyanol, and 0.1% bromophenol blue in 90% formamide. Before loading onto the gel, the reactions were denatured by heating at 100C° for 10 min and immediately transferred onto ice for 2 min. Products were resolved by denaturing PAGE (7 M urea and 15% acrylamide for 3 h at 2,000 V) and then visualized and quantified using a Molecular Dynamics PhosphorImager and ImageQuant software. Primer elongation was calculated as percent of total primer termini and plotted versus enzyme concentration.

To assay the processivity of pol η, primer extension reactions were performed by preincubating the pol alone or in the presence of MSH2–MSH6 with the labeled DNA template for 5 min at room temperature. A mixture of 1 μg herring sperm DNA (500 M excess) and 100 μM of all four dNTPs was then added to initiate the reaction. Reactions were terminated after 2 min by mixing with 10 μl of formamide loading dye and analyzed on a polyacrylamide gel. The effectiveness of the trap was confirmed by preincubating pol η with the DNA substrate and excess herring sperm DNA before the addition of the nucleotides (not depicted). The lack of DNA synthesis in this case verified that excess herring sperm DNA was sufficient to trap all pol molecules.

Kinetic analysis of replication products. The K_m and V_{max} for dTTP incorporation opposite template A were determined by measuring primer elongation as a function of nucleotide concentration as described previously (48). Preliminary studies demonstrated that <20% of the primers were extended to ensure steady-state conditions. 10 nM DNA substrates were replicated for 2 min at 37°C in reaction mixtures containing 5 nM pol η. The dTTP concentrations ranged from 0.5 to 32 μM. Reaction products were separated in a 20% polyacrylamide gel containing 7 M urea and then visualized and quantified using a PhosphorImager. The velocity of dNTP incorporation was determined by dividing the percent of product generated by the respective time of the reaction. The apparent V_{max} and K_m were determined from a Hanes-Woolf plot by linear least squares fit using the Sigma Plot software. The efficiency of nucleotide insertion by pol was calculated as V_{max}/K_m.

We thank David Wilson, Nik Joshi, James Carney, and Ranjan Sen for stimulating discussions; Xianmin Zeng, Cayetano von Kobbe, and Wen-Hsing Cheng for technical advice; Wendy Chang for making the GST-pol η expression plasmid, pWC9; William Yang for technical assistance; and Vilhelm Bohr for support.

This work was supported by the NIH intramural research program (to P.J. Gearhart and R. Woodgate) and NIH grant CA96590 (to T.M. Wilson).

The authors have no conflicting financial interests.

Submitted: 6 October 2004
Accepted: 8 December 2004

REFERENCES

1. Muramatsu, M., K. Kinoshita, S. Faragasan, S. Yamada, Y. Shinkai, and T. Honjo. 2000. Class switch recombination and hypermutation require activation-induced cytidine deaminase (AID), a potential RNA editing enzyme. *Cell.* 102:553–563.
2. Revy, P., T. Muto, Y. Levy, F. Geissmann, A. Piebani, O. Sanal, N. Catalan, M. Forveille, R. Dufourcq-Lagelouse, A. Gennery, et al. 2000. Activation-induced cytidine deaminase (AID) causes the autosomal recessive form of the hyper-IgM syndrome (HIGM2). *Cell.* 102: 565–575.
3. Bransteitter, R., P. Pham, M.D. Scharff, and M.F. Goodman. 2003. Activation-induced cytidine deaminase deaminates deoxycytidine on single-stranded DNA but requires the action of RNase. *Proc. Natl. Acad. Sci. USA.* 100:4102–4107.
4. Chaudhuri, J., M. Tian, C. Khuong, K. Chua, E. Pinaud, and F.W. Alt. 2003. Transcription-targeted DNA deamination by the AID antibody diversification enzyme. *Nature.* 422:726–730.
5. Ramiro, A.R., P. Stavropoulos, M. Jankovic, and M.C. Nussenzweig. 2003. Transcription enhances AID-mediated cytidine deamination by exposing single-stranded DNA on the nontemplate strand. *Nat. Immunol.* 4:452–456.
6. Dickerson, S.K., E. Market, E. Besmer, and F.N. Papavasiliou. 2003. AID mediates hypermutation by deaminating single stranded DNA. *J. Exp. Med.* 197:1291–1296.
7. Sohail, A., J. Klapacz, M. Samaranayake, A. Ullah, and A.S. Bhagwat. 2003. Human activation-induced cytidine deaminase causes transcription-dependent, strand-biased C to U deaminations. *Nucleic Acids Res.* 31:2990–2994.
8. Pham, P., R. Bransteitter, J. Petruska, and M.F. Goodman. 2003. Processive AID-catalysed cytosine deamination on single-stranded DNA simulates somatic hypermutation. *Nature.* 424:103–107.
9. Yu, K., F.T. Huang, and M.R. Lieber. 2004. DNA substrate length and surrounding sequence affect the activation induced deaminase activity at cytidine. *J. Biol. Chem.* 279:6496–6500.
10. Petersen-Mahrt, S.K., R.S. Harris, and M.S. Neuberger. 2002. AID mutates *E. coli* suggesting a DNA deamination mechanism for antibody diversification. *Nature.* 418:99–103.
11. Di Noia, J., and M.S. Neuberger. 2002. Altering the pathway of immunoglobulin hypermutation by inhibiting uracil-DNA glycosylase. *Nature.* 419:43–48.
12. Rada, C., G.T. Williams, H. Nilsen, D.E. Barnes, T. Lindahl, and M.S. Neuberger. 2002. Immunoglobulin isotype switching is inhibited and somatic hypermutation perturbed in UNG-deficient mice. *Curr.*

Biol. 12:1748–1755.
13. Imai, K., G. Slupphaug, W.I. Lee, P. Revy, S. Nonoyama, N. Catalan, L. Yel, M. Forveille, B. Kavli, H.E. Krokan, et al. 2003. Human uracil-DNA glycosylase deficiency associated with profoundly impaired immunoglobulin class-switch recombination. *Nat. Immunol.* 4:1023–1028.
14. Gearhart, P.J. 2002. The roots of antibody diversity. *Nature.* 419:29–30.
15. Lehmann, A.R. 2003. Replication of damaged DNA. *Cell Cycle.* 2:300–302.
16. Poltoratsky, V.P., S.H. Wilson, T.A. Kunkel, and Y.I. Pavlov. 2004. Recombinogenic phenotype of human activation-induced cytosine deaminase. *J. Immunol.* 172:4308–4313.
17. Yoshikawa, K., I. Odazaki, T. Eto, K. Kinoshita, M. Muramatsu, H. Nagaoka, and T. Honjo. 2002. AID enzyme-induced hypermutation in an actively transcribed gene in fibroblasts. *Science.* 296:2033–2036.
18. Martin, A., P.D. Bardwell, C.J. Woo, M. Fan, M.J. Shulman, and M.D. Scharff. 2002. Activation-induced cytidine deaminase turns on somatic hypermutation in hybridomas. *Nature.* 415:802–806.
19. Woo, C.J., A. Martin, and M.D. Scharff. 2003. Induction of somatic hypemutation is associated with modifications in immunoglobulin variable region chromatin. *Immunity.* 19:479–489.
20. Okazaki, I., H. Hiai, N. Kakazu, S. Yamada, M. Muramatsu, K. Kinoshita, and T. Honjo. 2003. Constitutive expression of AID leads to tumorigenesis. *J. Exp. Med.* 197:1173–1181.
21. Chaudhuri, J., C. Khuong, and F.W. Alt. 2004. Replication protein A interacts with AID to promote deamination of somatic hypermutation targets. *Nature.* 430:992–998.
22. Jacobs, H., Y. Fukita, G.T.J. van der Horst, J. de Boer, G. Weeda, J. Essers, N. de Wind, B.P. Engelward, L. Samson, S. Verbeek, et al. 1998. Hypermutation of immunoglobulin genes in memory B cells of DNA repair-deficient mice. *J. Exp. Med.* 187:1735–1743.
23. Phung, Q.H., D.B. Winter, A. Cranston, R.E. Tarone, V.A. Bohr, R. Fishel, and P.J. Gearhart. 1998. Increased hypermutation at G and C nucleotides in immunoglobulin variable genes from mice deficient in the MSH2 mismatch repair protein. *J. Exp. Med.* 187:1745–1751.
24. Frey, S., B. Bertocci, F. Delbos, L. Quint, J.C. Weill, and C.A. Reynaud. 1998. Mismatch repair deficiency interferes with the accumulation of mutations in chronically stimulated B cells and not with the hypermutation process. *Immunity.* 9:127–134.
25. Rada, C., M.R. Ehrenstein, M.S. Neuberger, and C. Milstein. 1998. Hot spot focusing of somatic hypermutation in MSH2-deficient mice suggests two stages of mutational targeting. *Immunity.* 9:135–141.
26. Wiesendanger, M., B. Kneitz, W. Edelmann, and M.D. Scharff. 2000. Somatic hypermutation in MutS homologue (MSH)3-, MSH6-, and MSH3/MSH6-deficient mice reveals a role for the MSH2-MSH6 heterodimer in modulating the base substitution pattern. *J. Exp. Med.* 191: 579–584.
27. Martin, A., Z. Li, D.P. Lin, P.D. Bardwell, M.D. Iglesias-Ussel, W. Edelmann, and M.D. Scharff. 2003. Msh2 ATPase activity is essential for somatic hypermutation at A-T basepairs and for efficient class switch recombination. *J. Exp. Med.* 198:1171–1178.
28. Li, Z., S.J. Scherer, D. Ronai, M.D. Iglesias-Ussel, J.U. Peled, P.D. Bardwell, M. Zhuang, K. Lee, A. Martin, W. Edelmann, and M.D. Scharff. 2004. Examination of Msh6- and Msh3-deficient mice in class switching reveals overlapping and distinct roles of MutS homologues in antibody diversification. *J. Exp. Med.* 200:47–59.
29. Martomo, S.A., W.W. Yang, and P.J. Gearhart. 2004. A role for Msh6 but not Msh3 in somatic hypermutation and class switch recombination. *J. Exp. Med.* 200:61–68.
30. Winter, D.B., Q.H. Phung, A. Umar, S.M. Baker, R.E. Tarone, K. Tanaka, R.M. Liskay, T.A. Kunkel, V.A. Bohr, and P.J. Gearhart. 1998. Altered spectra of hypermutation in antibodies from mice deficient for the DNA mismatch repair protein PMS2. *Proc. Natl. Acad. Sci. USA.* 95:6953–6958.
31. Phung, Q.H., D.B. Winter, R. Alrefai, and P.J. Gearhart. 1999. Hypermutation in Ig V genes from mice deficient in the MLH1 mismatch repair protein. *J. Immunol.* 162:3121–3124.
32. Kim, N., G. Bozek, J.C. Lo, and U. Storb. 1999. Different mismatch repair deficiencies all have the same effects on somatic hypermutation: intact primary mechanism accompanied by secondary modifications. *J. Exp. Med.* 190:21–30.
33. Ehrenstein, M.R., C. Rada, A.M. Jones, C. Milstein, and M.S. Neuberger. 2001. Switch junction sequences in PMS2-deficient mice reveal a microhomology-mediated mechanism of Ig class switch recombination. *Proc. Natl. Acad. Sci. USA.* 98:14553–14558.
34. Zeng, X., D.B. Winter, C. Kasmer, K.H. Kraemer, A.R. Lehmann, and P.J. Gearhart. 2001. DNA polymerase η is an A-T mutator in somatic hypermutation of immunoglobulin variable genes. *Nat. Immunol.* 2:537–541.
35. Faili, A., S. Aoufouchi, S. Weller, F. Vuillier, A. Stary, A. Sarasin, C.A. Reynaud, and J.C. Weill. 2004. DNA polymerase η is involved in hypermutation occurring during immunoglobulin class switch recombination. *J. Exp. Med.* 199:265–270.
36. Zeng, X., G.A. Negrete, C. Kasmer, W.W. Yang, and P.J. Gearhart. 2004. Absence of DNA polymerase η reveals targeting of C mutations on the nontranscribed strand in immunoglobulin switch regions. *J. Exp. Med.* 199:917–924.
37. Rogozin, I.B., Y.I. Pavlov, K. Bebenek, T. Matsuda, and T.A. Kunkel. 2001. Somatic mutation hotspots correlate with DNA polymerase η error spectrum. *Nat. Immunol.* 2:530–536.
38. Pavlov, Y.I., I.B. Rogozin, A.P. Galkin, A.Y. Aksenova, F. Hanaoka, C. Rada, and T.A. Kunkel. 2002. Correlation of somatic hypermutation specificity and A-T base pair substitution errors by DNA polymerase η during copying of a mouse immunoglobulin κ light chain transgene. *Proc. Natl. Acad. Sci. USA.* 99:9954–9959.
39. Esposito, G., G. Texido, U.A.K. Betz, H. Gu, W. Müller, U. Klein, and K. Rajewsky. 2000. Mice reconstituted with DNA polymerase β-deficient fetal liver cells are able to mount a T cell-dependent immune response and mutate their Ig genes normally. *Proc. Natl. Acad. Sci. USA.* 97:1166–1171.
40. Diaz, M., L.K. Verkoczy, M.F. Flajnik, and N.R. Klinman. 2001. Decreased frequency of somatic hypermutation and impaired affinity maturation but intact germinal center formation in mice expressing antisense RNA to DNA polymerase ζ. *J. Immunol.* 167:327–335.
41. Bertocci, B., A. de Smet, E. Flatter, A. Dahan, J.C. Bories, C. Landreau, J.C. Weill, and C.A. Reynaud. 2002. DNA polymerases μ and λ are dispensable for Ig gene hypermutation. *J. Immunol.* 168:3702–3706.
42. Schenten, D., V.L. Gerlach, C. Guo, S. Velasco-Miguel, C.L. Hladik, C.L. White, E.C. Friedberg, K. Rajewsky, and G. Esposito. 2002. DNA polymerase κ deficiency does not affect somatic hypermutation in mice. *Eur. J. Immunol.* 32:3152–3160.
43. McDonald, J.P., E.G. Frank, B.S. Plosky, I.B. Rogozin, C. Masutani, F. Hanaoka, R. Woodgate, and P.J. Gearhart. 2003. 129-derived strains of mice are deficient in DNA polymerase ι and have normal immunoglobulin hypermutation. *J. Exp. Med.* 198:635–643.
44. Gu, L., J. Wu, L. Qiu, C.D. Jennings, and G.M. Li. 2002. Involvement of DNA mismatch repair in folate deficiency-induced apoptosis. *J. Nutr. Biochem.* 13:355–363.
45. Faili, A., S. Aoufouchi, E. Flatter, Q. Guéranger, C.-A. Reynaud, and J.-C. Weill. 2002. Induction of somatic hypermutation in immunoglobulin genes is dependent on DNA polymerase iota. *Nature.* 419:944–947.
46. McCulloch, S.D., R.J. Kokoska, C. Masutani, S. Iwai, F. Hanaoka, and T.A. Kunkel. 2004. Preferential *cis-syn* thymine dimer bypass by DNA polymerase η occurs with biased fidelity. *Nature.* 428:97–100.
47. Masutani, C., R. Kusumoto, S. Iwai, and F. Hanaoka. 2000. Mechanisms of accurate translesion synthesis by human DNA polymerase η. *EMBO J.* 19:3100–3109.
48. Creighton, S., L.B. Bloom, and M.F. Goodman. 1995. Gel fidelity assay measuring nucleotide misinsertion, exonucleolytic proofreading, and lesion bypass efficiencies. *Methods Enzymol.* 262:232–256.
49. Leeds, J.M., M.B. Slabaugh, and C.K. Mathews. 1985. DNA precursor pools and ribonucleotide reductase activity: distribution between the nucleus and cytoplasm of mammalian cells. *Mol. Cell. Biol.* 5:3443–3450.
50. Lan, L., T. Hayashi, R.M. Rabeya, S. Nakajima, S. Kanno, M. Takao, T. Matsunaga, M. Yoshino, M. Ichikawa, H. te Riele, et al. 2004. Functional and physical interactions between ERCC1 and MSH2

complexes for resistance to cis-diamminedichloroplatinum(II) in mammalian cells. *DNA Repair (Amst.).* 3:135–143.
51. Schrader, C.E., J. Vardo, E. Linehan, M.Z. Twarog, L.J. Niedernhofer, J.H.J. Hoeijmakers, and J. Stavnezer. 2004. Deletion of the nucleotide excision repair gene *Ercc1* reduces immunoglobulin class switching and alters mutations near switch recombination junctions. *J. Exp. Med.* 200:321–330.
52. Gaudreault, I., D. Guay, and M. Lebel. 2004. YB-1 promotes strand separation in vitro of duplex DNA containing either mispaired bases or cisplatin modifications, exhibits endonucleolytic activities and binds several DNA repair proteins. *Nucleic Acids Res.* 32:316–327.
53. Schmutte, C., R.C. Marinescu, M.M. Sadoff, S. Guerrete, J. Overhauser, and R. Fishel. 1998. Human exonuclease I interacts with the mismatch repair protein hMSH2. *Cancer Res.* 58:4537–4542.
54. Bardwell, P.D., C.J. Woo, K. Wei, Z. Li, A. Martin, S.Z. Sack, T. Parris, W. Edelmann, and M.D. Scharff. 2004. Altered somatic hypermutation and reduced class-switch recombination in exonuclease 1-mutant mice. *Nat. Immunol.* 5:224–229.
55. Rada, C., J.M. Di Noia, and M.S. Neuberger. 2004. Mismatch recognition and uracil-excision provide complementary paths to both Ig switching and the A/T-focused phase of somatic mutation. *Mol. Cell.* 16:163–171.
56. Wilson, T., S. Guerrette, and R. Fishel. 1999. Dissociation of mismatch recognition and ATPase activity by hMSH2-hMSH3. *J. Biol. Chem.* 274:21659–21664.
57. Gradia, S., S. Acharya, and R. Fishel. 1997. The human mismatch recognition complex hMSH2-hMSH6 functions as a novel molecular switch. *Cell.* 91:995–1005.
58. Kannouche, P., B.C. Broughton, M. Volker, F. Hanaoka, L.H.F. Mullenders, and A.R. Lehmann. 2001. Domain structure, localization, and function of DNA polymerase η, defective in xeroderma pigmentosum variant cells. *Genes Dev.* 15:158–172.
59. Kannouche, P., A.R. Fernández de Henestrosa, B. Coull, A.E. Vidal, C. Gray, D. Zicha, R. Woodgate, and A.R. Lehmann. 2003. Localization of DNA polymerase η and ι to the replication machinery is tightly co-ordinated in human cells. *EMBO J.* 22:1223–1233.
60. Tissier, A., J.P. McDonald, E.G. Frank, and R. Woodgate. 2000. Pol ι, a remarkably error-prone human DNA polymerase. *Genes Dev.* 14: 1642–1650.
61. Brosh, R.M., Jr., J.L. Li, M.K. Kenny, J.K. Karow, M.P. Cooper, R.P. Kureekattil, I.D. Hickson, and V.A. Bohr. 2000. Replication protein A physically interacts with the Bloom's syndrome protein and stimulates its helicase activity. *J. Biol. Chem.* 275:23500–23508.
62. Niwa, H., K. Yamamura, and J. Miyazaki. 1991. Efficient selection for high-expression transfectants with a novel eukaryotic vector. *Gene.* 108:193–199.